

## Research



**Cite this article:** Rasmussen MH, Holler KR, Baio JE, Jaye C, Fischer DA, Gorb SN, Weidner T. 2022 Evidence that gecko setae are coated with an ordered nanometre-thin lipid film.

*Biol. Lett.* **18**: 20220093.

<https://doi.org/10.1098/rsbl.2022.0093>

Received: 21 February 2022

Accepted: 9 June 2022

### Subject Areas:

biochemistry, bioengineering

### Keywords:

adhesion, toe pad, reptiles, integument, spectro-microscopy, biotribology

### Author for correspondence:

Tobias Weidner

e-mail: [weidner@chem.au.dk](mailto:weidner@chem.au.dk)

Electronic supplementary material is available online at <https://doi.org/10.6084/m9.figshare.c.6049219>.

# Evidence that gecko setae are coated with an ordered nanometre-thin lipid film

Mette H. Rasmussen<sup>1</sup>, Katinka Rønnow Holler<sup>1</sup>, Joe E. Baio<sup>2</sup>, Cherno Jaye<sup>3</sup>, Daniel A. Fischer<sup>3</sup>, Stanislav N. Gorb<sup>4</sup> and Tobias Weidner<sup>1</sup>

<sup>1</sup>Department of Chemistry, Aarhus University, 8000 Aarhus C, Denmark

<sup>2</sup>The School of Chemical, Biological and Environmental Engineering, Oregon State University, Corvallis, OR, USA

<sup>3</sup>Material Measurement Laboratory, National Institute of Standards and Technology, Gaithersburg, MD, USA

<sup>4</sup>Department of Functional Morphology and Biomechanics, Institute of Zoology, Kiel University, Kiel, Germany

SNG, 0000-0001-9712-7953; TW, 0000-0002-7083-7004

The fascinating adhesion of gecko to virtually any material has been related to surface interactions of myriads of spatula at the tips of gecko feet. Surprisingly, the molecular details of the surface chemistry of gecko adhesion are still largely unknown. Lipids have been identified within gecko adhesive pads. However, the location of the lipids, the extent to which spatula are coated with lipids, and how the lipids are structured are still open questions. Lipids can modulate adhesion properties and surface hydrophobicity and may play an important role in adhesion. We have therefore studied the molecular structure of lipids at spatula surfaces using near-edge X-ray absorption fine structure imaging. We provide evidence that a nanometre-thin layer of lipids is present at the spatula surfaces of the tokay gecko (*Gekko gecko*) and that the lipids form ordered, densely packed layers. Such dense, thin lipid layers can effectively protect the spatula proteins from dehydration by forming a barrier against water evaporation. Lipids can also render surfaces hydrophobic and thereby support the gecko adhesive system by enhancement of hydrophobic–hydrophobic interactions with surfaces.

## 1. Introduction

Geckos have the fascinating ability to climb nearly every surface in almost any condition. As a consequence, gecko adhesion has inspired a long list of biomimetic applications in adhesion technologies [1–9]. Gecko toepads are equipped with a hair-like fine structure of setal arrays (figure 1). Each seta is terminated with bundles of spatula shafts, which are each tipped with a flat spatula at the end, which makes the adhesive contact to the surface [1,2,10–19] (figure 1). The setae branches originate from the outer epidermal layer of the gecko pad scales, the oberhautchen and the beta-layer [1,20]. The setal arrays are mainly comprised of  $\beta$ -proteins, which provide the tissue rigidity needed for constant attachment and detachment. Earlier studies have characterized setal proteins as  $\beta$ -keratins [21–23]. Studies by Alibardi and others found that the proteinaceous component of setae also consists of corneous  $\beta$ -proteins [22–27].

The mechanism of gecko adhesion has been in the strong focus of biomechanics and material science research for the last two decades. Some studies [2,3] concluded that the attraction of gecko setae to surfaces is driven by van der Waals interactions, while another showed a prominent role of water<sup>13</sup>. Within these scenarios, setae surface chemistry has long been ignored as likely to be of minor importance. Consequently, the detailed surface chemistry of gecko toepads is still largely unknown. More recent models of gecko adhesion now indicate that chemistry cannot be ignored and that chemical details matter for gecko surface adhesion. Vibrational surface spectroscopy

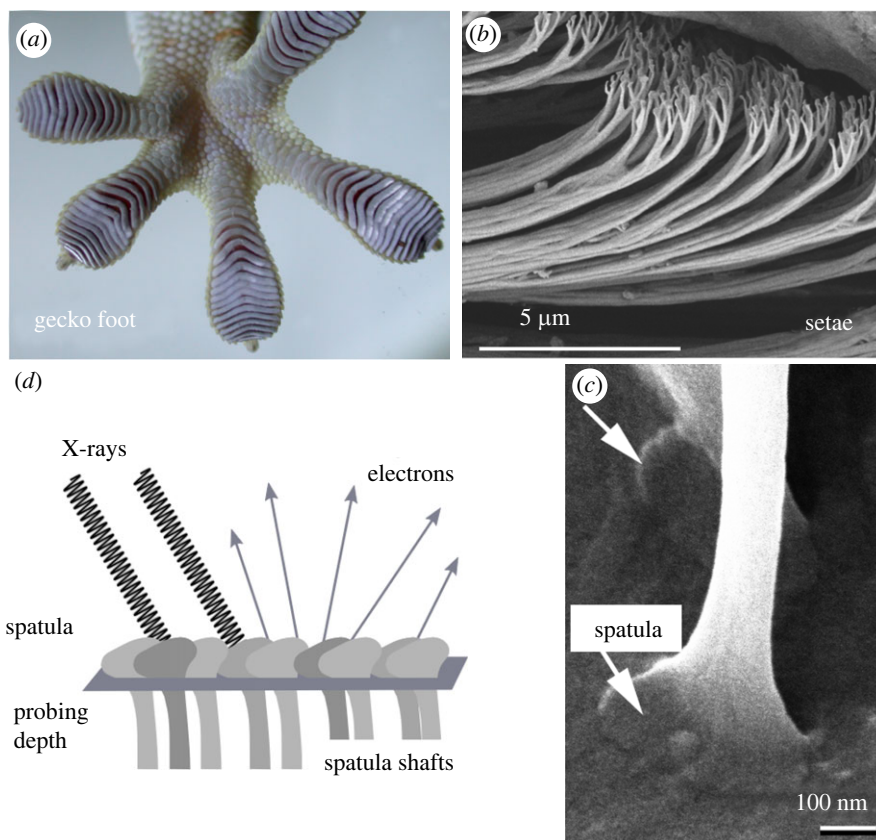


**Figure 1.** Gecko adhesive system and experimental geometry. (a) Photograph of a gecko toepad attached to a glass surface. The setal arrays are visible. (b) SEM image of the setal arrays. The terminal spatulae shafts and spatula form the contact with the surface. (c) Spatula in contact with a surface. (d) Experimental geometry. With a probing depth of 5–10 nm, the recorded images are representative of the spatula surface.

and nuclear magnetic resonance (NMR) indicate an important role of lipids and acid–base interactions for gecko adhesion [28–30]. As in any adhesion phenomenon, the outermost molecular structure of the setae defines the mechanical and chemical contact during adhesion. Detailed information about the chemical state of the seta surface can inform future biomimetic approaches.

Recently, it has been observed that gecko setae arrays have lipids associated with them [24]. Lipids are known to reside in the epidermis of reptiles in a ‘brick and mortar’ pattern [28,31]. Lipids have also been observed in gecko footprints [29], within setae [32] and at the surface of setae tissue [21,28,30]. This led Jain *et al.* [28] to propose a model, which stated that, along with a lipid coating leaving a footprint with each step, lipids are stored inside the setae. Lipids are known to have an important role in various biological systems, including the epidermis of mammalian, reptiles and avian species, where they among other things function as a water barrier [33–36]. Lipids have also been shown to have a role in the self-assembly of proteins in mussel byssal threads and thereby assist the adhesive properties of mussels [37]. Also, insects produce lipid-containing secretions in the contact region, to enhance adhesion [38–40]. Lipids could potentially render the proteinaceous setal tissue hydrophobic, which is often the basis for self-cleaning structures [41–44], and could thereby support such properties of gecko setae [45]. Lipids have also been found to be involved in surface adhesion via acid–base mechanisms [30].

We here used partial electron yield (PEY) near-edge X-ray absorption fine structure (NEXAFS) imaging (figure 1) to explore the chemical structure of the setae lipid coating of

the tokay gecko (*Gekko gecko*). For NEXAFS spectroscopy, the surface is irradiated with X-rays at photon energies near an ionization edge [46]. The emitted electrons are detected. When the incident photon energy is in resonance with a transition of core level electrons into unoccupied molecular orbitals near the ionization edge, the electron yield is enhanced. The intensity is also dependent on the relative orientation of the incoming X-rays and the respective transition dipole moment, which allows the molecular alignment and orientation to be probed [47]. In this study, we probed molecular orbitals near the carbon K-edge and the nitrogen K-edge.

Only electrons above a certain threshold energy are detected, which come from molecules near the material surface and NEXAFS spectroscopy is therefore a very surface sensitive method with a probing depth of approximately 5–10 nm [48]. For the imaging modality of NEXAFS spectroscopy we use here, the X-ray beam is widened to the size of the sample using a dithering mirror. The position of the electron emission is registered with a CCD camera coating (experimental procedures are outlined in the electronic supplementary material). Regular NEXAFS spectroscopy is challenging for charging and rough surfaces such as sum materials and especially animal surfaces. The NEXAFS microscopy used here is unaffected by charging and surface curvature. The NEXAFS microscope has been used previously to map the surface chemistries of car tires and multiplexing the analysis of surface coatings [49–51]. For this reason, NEXAFS imaging is also ideally suited to study complex surfaces such as animal surfaces and has been used to investigate the surface chemistry of snake scales, beetle cuticle and springtail surfaces [19,31,52,53].

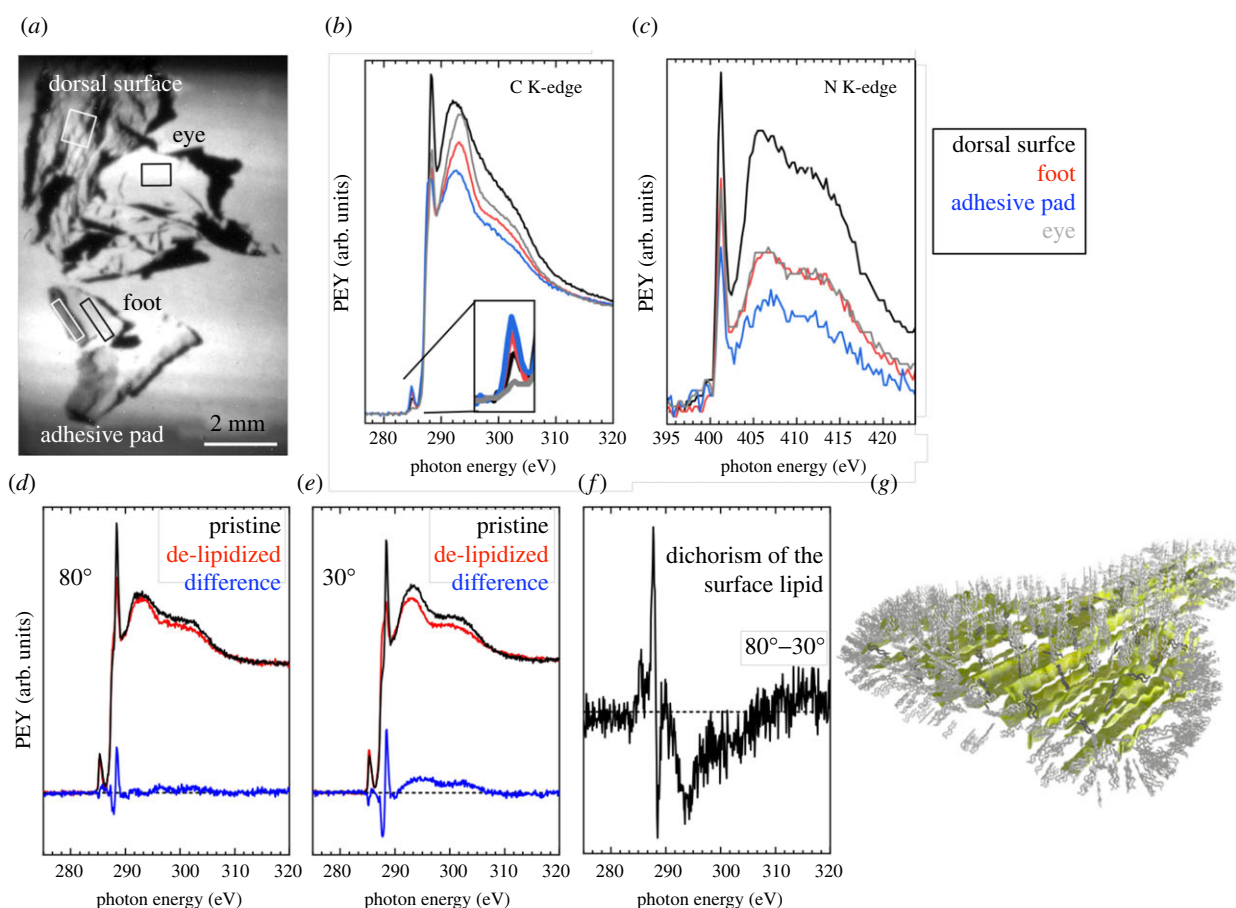


**Figure 2.** NEXAFS spectra of setae arrays and reference gecko tissue. (a) NEXAFS image of the PEY integrated over the entire nitrogen K-edge. The image shows the different types of tissue glued to the sample holder with copper tape. The image was recorded at a NEXAFS incidence angle of  $30^\circ$ . A full NEXAFS spectrum can be extracted from each pixel within the image. The ROI for the extraction of spectra for the setae array and other tissues for comparison (dorsal scales of the body, dorsal scales of the foot and eyelid scales) are indicated as boxes in black and white. (b) Carbon K-edge NEXAFS spectra were extracted from NEXAFS images of the setae arrays as well as the gecko scale tissue. (c) Nitrogen K-edge NEXAFS spectra extracted from the same ROIs as the carbon spectra. (d,e) NEXAFS C K-edge spectra of adhesive pads before and after lipid removal were extracted from images recorded with  $80^\circ$  (near-normal) and  $30^\circ$  (glancing) X-ray incidence angles. The difference spectra are representative of the lipid coating. (f) Difference spectrum of the difference spectra are shown in (a) and (b). The spectrum shows the angle dependence of the difference spectra in (a) and (b) and provides information about the orientation of lipids. (g) Schematic of a spatula and the lipid orientation determined from the spectrum shown in (f). Flat protein sheets (yellow) are covered and infused with lipids (grey).

## 2. Results and discussion

The carbon K-edge and nitrogen K-edge NEXAFS spectra of gecko setae arrays and three types of reference tissues (dorsal scales of the body, dorsal scales of the foot and eyelid scales) are shown in figure 2. The tissue samples have been attached to the sample holder using copper tape and then imaged using a NEXAFS microscope. The advantage of using the imaging modality of NEXAFS spectroscopy in the context of tissue analysis is that the microscope is based on a magnetic solenoid transmission of the special electron yield and channel plate imaging for electron detection, which provides a method to probe curved, non-conducting samples without spectral distortion [49].

The NEXAFS spectra displayed in figure 2b were extracted from the imaging data by plotting the PEY against the photon energy for four regions of interest (ROIs). The spectra for the different types of tissue are similar. All spectra exhibit an aliphatic  $\sigma^*$  resonance near 292 eV as well as C=C and C=O  $\pi^*$  resonances near 285 eV and 288 eV, respectively. These spectral features are expected for gecko skin samples containing complex biomolecules and the spectral shapes resemble those of lipids and proteins [54,55]. When comparing the composition of lipids and proteins, classes of biomolecules expected at

setae surfaces, proteins have a larger C=O content compared with lipids. The larger protein C=O content is also reflected in a higher C=O intensity in literature NEXAFS spectra [55–57]. For the gecko tissue samples, the C=O intensity is somewhat smaller at the setae surface, indicating a slightly larger amount of lipids covering the protein structure compared with the other tissue samples (see electronic supplementary material, figure S1 for intensities).

The C=C  $\pi^*$  resonances are relatively strong at the dorsal foot-related locations and weaker at the eyelid and the dorsal body scale, which could suggest that proteins in the dorsal foot scales and setae consist of a larger amount of aromatic amino acids (e.g. tyrosine). Studies by Rizzo *et al.* [20] showed the presence of tyrosine in the setae using Raman spectroscopy, but no similar studies have been conducted on the scales of the body, the foot and the eyelid.

The corresponding pre-edge normalized nitrogen K-edge NEXAFS spectra can be seen in figure 2c. The nitrogen spectra contain an amide  $\pi^*$  resonance near 401 eV, typically found in protein spectra, along with  $\sigma^*$  resonances above 405 eV, related to N–C and N–H containing groups in the backbone and side chains of proteins [54,58,59]. Lipids can also contain nitrogen species and certain lipids, such as sphingomyelin also contain amide groups, could interfere

with the protein amide spectra. Therefore, in order to identify the specific contribution of lipids within the nitrogen spectra, reference measurements were collected from samples, which were de-lipidized using published procedures (see electronic supplementary material, figure S2). Samples with lipids removed showed no significant difference compared with the native gecko tissue and, therefore, a significant lipid contribution to the amide signal can be excluded. As a result, the spectral features are likely related to  $\beta$ -proteins within the gecko tissue. At the specific PEY electron retardation voltage of  $-50$  V used in our NEXAFS experiments, the NEXAFS sampling depth can be expected to be 5 nm [48,60]. Since a nitrogen signal is detected, NEXAFS is evidently probing through the lipid layer into the spatulae protein matrix (figure 1 for illustration of the sampling depth relative to the tissue setal structures). This implies that the layer of lipids at the surface of the spatulae must be thinner than the sampling depth and therefore only up to 5 nm thin. The protein signal is strongest for the dorsal body scales, slightly lower for the dorsal foot scales and eyelid scales and lowest for the adhesive pad. In view of the already thin lipid coating on the setal arrays, the dorsal foot and eyelid tissue may have very few lipids at their surfaces.

Assuming the lipids are maintained as a functional layer in between shedding cycles, the question arises, how the lipid layer is replenished during locomotion. Hsu *et al.* [29] have reported lipids within gecko footprints using sum frequency generation spectroscopy. The detection limit of this method is on the order of single molecular layers so one can assume the at least a monolayer of lipids can be found within each footprint. Based on the NEXAFS results, this is on the same order as the coating of the setal array, which means the lipid layer must be replenished with every step. At a step rate of 10 Hz for a running gecko, the surface of the spatula must be recoated within 100 ms. To coat the surface area of the spatula of approximately  $2 \times 10^5 \text{ nm}^2$  via surface diffusion across the spatula shaft with a diameter of 100 nm and a diffusion coefficient of approximately  $10^{-8} \text{ cm}^2 \text{ s}^{-1}$ , based on lipid surface diffusion in lipid bilayers, [61] the replacement would require approximately 250 ms, which would be too slow for replenishment of the spatula lipid coating. Replenishment of lipids between detachment and reattachment via bulk diffusion through the volume of the setal tissue would also be in agreement with recently published NMR data, which indicated that lipids are also present within the setae tissue [28]. There are large uncertainties involved in the estimation of the surface diffusion coefficient since only limited theoretical and experimental diffusion data are available and most of the available diffusion coefficients have been determined for phospholipid diffusion within lipid bilayers and monolayers. A detailed understanding of lipid replenishment will therefore require measurements of the surface diffusion constants of the lipids across proteinaceous surfaces for the lipids identified on setae surfaces. In this sense, based on our data we cannot rule out surface diffusion as an important mechanism. It is also possible, that both surface and bulk diffusion processes play a role and provide a robust mechanism for lipid replenishment for the gecko adhesive system. Particularly given the strong dependence of the diffusion process on additional environmental factors such as temperature and spatula dynamics, the high melting point of lipids involved, which can severely impede lipid transport across the spatula shaft surface.

Both the structure and orientation of the lipid coating can be identified using angle-resolved NEXAFS spectroscopy. For these experiments, we compare native setae with samples, which have been de-lipidized as reference using established procedures. To record spectra of the lipid coating, the reference spectrum was subtracted from the native spectra. Samples and references were mounted on the same sample holder and imaged together. The spectra extracted from the ROI covering the native and de-lipidized setae are shown in figure 2*d* for NEXAFS sample angles of  $80^\circ$  (near-normal, electric field in sample plane). Figure 2*e* displays spectra for the native and de-lipidized setae recorded at  $30^\circ$  (glancing, electric field near perpendicular to sample plane). The difference (blue) of the spectra related to the native (black) and de-lipidized (red) samples for each angle are representative of the lipids coating of the spatula. As seen for the other tissue samples, resonances related to aromatic groups, carbon double bonds as well as alkyl chains and carboxyl moieties are all visible.

As evident from the negative polarity of the resonance near 286.7 eV for both angles, in relation to the total carbon content, there are fewer C–H groups present in the lipid coating than in the underlying keratin layer, while C=O and C–C are higher in intensity on the native sample. The relative amounts of C–H and C=O binding agrees well with the hypothesis that lipids are removed as lipids have a higher relative number of C–H groups and a lower number of C=O groups compared with proteins.

The orientation and ordering of molecular bonds can be determined by following changes in the X-ray absorption as we change the angle of the sample with respect to the incident X-rays. By taking the difference of the difference spectra in figure 2*a,b*, we can specifically determine the angle dependence, i.e. the NEXAFS dichroism, of the lipid layer. The dichroism spectrum of the lipid layer is shown in figure 2*f*. By considering the relative orientations of the incoming X-rays and the molecular orbitals, as shown in the supporting information, the orientation of the lipids can be determined. The difference spectrum of the lipid layer in figure 2*f* exhibits a positive dichroism for the  $\pi^*(\text{C}=\text{C})$  and  $\sigma^*(\text{C}-\text{H})$  resonances. The  $\pi^*$  resonance related to C=O bonds and the  $\sigma^*(\text{C}-\text{C})$  features are negative. The difference spectrum demonstrates a high degree of ordering of alkyl chains and carboxyl moieties at the surface, as expected for an ordered lipid layer. For this specific experiment, only the outermost section of the adhesive pad is sampled, which is coated with lipids. Therefore, the dichroism can be used to determine the orientation of the lipids based on the polarity of the difference peaks. As evident from the orientation of the bonds relative to the alkyl chains (see supporting information for a schematic drawing of bonds), a positive dichroism for C=C and C–H bonds with a negative dichroism for C=O and C–C bonds is the signature of an upright orientation of the lipid alkyl chains.

A schematic model of the lipid structure relative to the geometry of the protein backbone proposed in [19] is shown in figure 2*g*. Based on the upright lipid orientation, an average length of lipid of about 2 nm and a maximum layer thickness of 5 nm, we can estimate that the lipid film consists of three lipid layers. The exact thickness cannot be inferred from the data and is therefore depicted only schematically in figure 2*g*. However, thickness and orientation estimates are very close to what Singla *et al.* have proposed

based on sum frequency generation experiments of setae attached to sapphire [30].

### 3. Conclusion

While, at this point, we can only speculate about the function of the lipid layer, interfacial lipids could have several potential advantages for adhesion. Singla *et al.* recently proposed that lipids could support adhesion to sapphire surfaces by an acid–base mechanism [30]. The lipid layer may also be involved in keeping the proteins of setae and spatulae hydrated by enclosing the proteinaceous tissue and thereby reducing water evaporation. It has previously been shown that dried out gecko setae adhere stronger when they are under high humidity (hydrated) conditions [13]. This might be due to the lower elasticity modulus of setae in hydrated condition, which leads to the enhancement of the contact formation with the nanoscale roughness. This effect may be similar to the role of lipids at insect setae, where lipids prevent the drying out of resilin (rubber-like protein with hydrogel properties, which is present at the setal tips) [38].

The polarity of a surface can play an important role for adhesion and lipids can render the proteinaceous spatula surfaces hydrophobic. Hydrophobic–hydrophobic interactions with the substrate can be rather strong, and many substrates for tokay gecko are relatively hydrophobic, including the vast majority of plant surfaces. Also, hydrophobic array of seta may lead to de-wetting of substrates covered by fluid water by using trapped air bubbles between setae [9,41]. The self-cleaning property of setae, [44,45] especially in the case of hydrophilic dust particles, and their ability to rapidly remove water from wet toe pads might be supported by the hydrophobic properties of the setal arrays.

In summary, we find that gecko setae are covered with a nanometre-thin layer of ordered lipids. The lipids are oriented upright, which indicates high density and alignment. The replenishment and function of the lipid coating

remain open questions, which could be addressed by future experiments combining spectroscopy with functional studies.

**Data accessibility.** NEXAFS imaging data are available for download on figshare.com under doi:10.6084/m9.figshare.19825246. The imaging data can be accessed using the LDF software, which can be obtained from Synchrotron Research, Inc. A license from Synchrotron Research is required to use the software.

The data are provided in the electronic supplementary material [62].

**Authors' contributions.** M.H.R.: conceptualization, data curation, formal analysis, writing—original draft and writing—review and editing; K.R.H.: data curation, formal analysis, investigation, writing—original draft and writing—review and editing; J.E.B.: conceptualization, data curation, formal analysis, funding acquisition, investigation, methodology, supervision, validation, writing—original draft and writing—review and editing; C.J.: data curation, formal analysis, investigation and writing—review and editing; D.A.F.: formal analysis, investigation, software and writing—review and editing; S.N.G.: formal analysis, investigation, methodology, writing—original draft and writing—review and editing; T.W.: conceptualization, data curation, formal analysis, funding acquisition, investigation, methodology, project administration, supervision, validation, writing—original draft and writing—review and editing.

All authors gave final approval for publication and agreed to be held accountable for the work performed therein.

**Conflict of interest declaration.** We declare we have no competing interests.

**Funding.** T.W. and M.H.R. thank the Danmarks Frie Forskningsfond (grant no. DFF FNU 8021-00046B) for financial support. J.E.B. thanks the National Science Foundation for a research fellowship (NSF grant no. 1202620). S.N.G. was supported by the German Science Foundation (project no. DFG GO 995/38-1). This work was performed at the NLSL, Brookhaven National Laboratory, which is supported by the US Department of Energy under contract no. DE-AC02-98CH10886. Research was performed at the National Institute of Standards and Technology (NIST) beamline SST-1 of the National Synchrotron Light Source II, a US Department of Energy (DOE) Office of Science User Facility operated for the DOE Office of Science by Brookhaven National Laboratory (New York, United States) under contract no. DE-SC0012704.

**Acknowledgement.** We thank Marianne Meijer of Kerncraft Art and Graphics for 3D visualizations. Certain commercial names are mentioned in this manuscript for the purposes of example and do not represent an endorsement by the National Institute of Standards and Technology.

### References

- Hiller U. 1968 Untersuchungen zum Feinbau und zur Funktion der Haftborsten von Reptilien. *Z. Morphol. Tiere* **62**, 307–362. (doi:10.1007/BF00401561)
- Autumn K, Liang YA, Hsieh ST, Zesch W, Chan WP, Kenny TW, Fearing R, Full RJ. 2000 Adhesive force of a single gecko foot-hair. *Nature* **405**, 681–685. (doi:10.1038/35015073)
- Autumn K. 2006 How gecko toes stick: the powerful, fantastic adhesive used by geckos is made of nanoscale hairs that engage tiny forces, inspiring envy among human imitators. *Am. Sci.* **94**, 124–133. (doi:10.1511/2006.58.124)
- Jagota A, Bennison SJ. 2002 Mechanics of adhesion through a fibrillar microstructure. *Integr. Comp. Biol.* **42**, 1140–1145. (doi:10.1093/icb/42.6.1140)
- Northern MT, Turner KL. 2005 A batch fabricated biomimetic dry adhesive. *Nanotechnology* **16**, 1159–1166. (doi:10.1088/0957-4484/16/8/030)
- Yurdumakan B, Ravivakar NR, Ajayan PM, Dhinojwala A. 2005 Synthetic gecko foot-hairs from multiwalled carbon nanotubes. *Chem. Commun.* 3799–3801. (doi:10.1039/b506047h)
- Niewiarowski PH, Lopez S, Ge L, Hagan E, Dhinojwala A. 2008 Sticky gecko feet: the role of temperature and humidity. *PLoS ONE* **3**, e2192. (doi:10.1371/journal.pone.0002192)
- Niewiarowski PH, Stark AY, Dhinojwala A. 2016 Sticking to the story: outstanding challenges in gecko-inspired adhesives. *J. Exp. Biol.* **219**, 912–919. (doi:10.1242/jeb.080085)
- Tan D *et al.* 2020 Humidity-modulated core–shell nanopillars for enhancement of gecko-inspired adhesion. *ACS Appl. Nano Mater.* **3**, 3596–3603. (doi:10.1021/acsnm.0c00314)
- Huber G, Gorb SN, Spolenak R, Arzt E. 2005 Resolving the nanoscale adhesion of individual gecko spatulae by atomic force microscopy. *Biol. Lett.* **1**, 2–4. (doi:10.1098/rsbl.2004.0254)
- Arzt E, Gorb SN, Spolenak R. 2003 From micro to nano contacts in biological attachment devices. *Proc. Natl Acad. Sci. USA* **100**, 10 603–10 606. (doi:10.1073/pnas.1534701100)
- Persson BNJ, Gorb S. 2003 The effect of surface roughness on the adhesion of elastic plates with application to biological systems. *J. Chem. Phys.* **119**, 11 437–11 444. (doi:10.1063/1.1621854)
- Huber G, Mantz H, Spolenak R, Mecke K, Jacobs K, Gorb SN, Arzt E. 2005 Evidence for capillarity contributions to gecko adhesion from single spatula nanomechanical measurements. *Proc. Natl Acad. Sci. USA* **102**, 16 293–16 296. (doi:10.1073/pnas.0506328102)
- Huber G, Gorb SN, Hosoda N, Spolenak R, Arzt E. 2007 Influence of surface roughness on gecko adhesion. *Acta Biomater.* **3**, 607–610. (doi:10.1016/j.actbio.2007.01.007)
- Spolenak R, Gorb S, Gao H, Arzt E. 2005 Effects of contact shape on the scaling of biological

- attachments. *Proc. R. Soc. A* **461**, 305–319. (doi:10.1098/rspa.2004.1326)
16. Varenberg M, Pugno NM, Gorb SN. 2010 Spatulate structures in biological fibrillar adhesion. *Soft Matter* **6**, 3269–3272. (doi:10.1039/c003207g)
  17. Filippov A, Popov VL, Gorb SN. 2011 Shear induced adhesion: contact mechanics of biological spatula-like attachment devices. *J. Theor. Biol.* **276**, 126–131. (doi:10.1016/j.jtbi.2011.01.049)
  18. Filippov AE, Gorb SN. 2015 Spatial model of the gecko foot hair: functional significance of highly specialized non-uniform geometry. *Interface Focus* **5**, 20140065. (doi:10.1098/rsfs.2014.0065)
  19. Holler KR, Rasmussen MA, Baio JE, Jaye C, Fischer DA, Gorb SN, Weidner T. 2022 Structure of keratins in adhesive gecko setae determined by near-edge X-ray absorption fine structure spectromicroscopy. *J. Phys. Chem. Lett.* **13**, 2193–2196. (doi:10.1021/acs.jpcclett.2c00004)
  20. Rizzo NW, Gardner KH, Walls DJ, Keiper-Hrynko NM, Ganzke TS, Hallahan DL. 2006 Characterization of the structure and composition of gecko adhesive setae. *J. R. Soc. Interface* **3**, 441–451. (doi:10.1098/rsif.2005.0097)
  21. Hallahan DL, Keiper-Hrynko NM, Shang TQ, Ganzke TS, Toni M, Dalla Valle L, Alibardi L. 2009 Analysis of gene expression in gecko digital adhesive pads indicates significant production of cysteine- and glycine-rich beta-keratins. *J. Exp. Zool. B* **312**, 58–73. (doi:10.1002/jez.b.21242)
  22. Alibardi L. 2013 Immunolocalization of keratin-associated beta-proteins (beta-keratins) in pad lamellae of geckos suggest that glycine-cysteine-rich proteins contribute to their flexibility and adhesiveness. *J. Exp. Zool. A* **319**, 166–178. (doi:10.1002/jez.1782)
  23. Alibardi L. 2018 Review: mapping proteins localized in adhesive setae of the tokay gecko and their possible influence on the mechanism of adhesion. *Protoplasm* **255**, 1785–1797. (doi:10.1007/s00709-018-1270-9)
  24. Alibardi L, Edward DP, Patil L, Bouhenni R, Dhinojwala A, Niewiarowski PH. 2011 Histochemical and ultrastructural analyses of adhesive setae of lizards indicate that they contain lipids in addition to keratins. *J. Morphol.* **272**, 758–768. (doi:10.1002/jmor.10948)
  25. Calvaresi M, Eckhart L, Alibardi L. 2016 The molecular organization of the beta-sheet region in corneous beta-proteins (beta-keratins) of sauropsids explains its stability and polymerization into filaments. *J. Struct. Biol.* **194**, 282–291. (doi:10.1016/j.jsb.2016.03.004)
  26. Wang F, Chen M, Cai F, Li P, Yan J, Zhou K. 2020 Expression of specific corneous beta proteins in the developing digits of the Japanese gecko (*Gekko japonicus*) reveals their role in the growth of adhesive setae. *Comp. Biochem. Physiol. B* **240**, 110370. (doi:10.1016/j.cbpb.2019.110370)
  27. Gamble T. 2019 Duplications in corneous beta protein genes and the evolution of gecko adhesion. *Integr. Comp. Biol.* **59**, 193–202. (doi:10.1093/icb/icz010)
  28. Jain D, Stark AY, Niewiarowski PH, Miyoshi T, Dhinojwala A. 2015 NMR spectroscopy reveals the presence and association of lipids and keratin in adhesive gecko setae. *Sci. Rep.* **5**, 9594. (doi:10.1038/srep09594)
  29. Hsu PY, Ge L, Li X, Stark AY, Wesdemiotis C, Niewiarowski PH, Dhinojwala A. 2012 Direct evidence of phospholipids in gecko footprints and spatula–substrate contact interface detected using surface-sensitive spectroscopy. *J. R. Soc. Interface* **9**, 657–664. (doi:10.1098/rsif.2011.0370)
  30. Singla S, Jain D, Zoltowski Chelsea M, Voleti S, Stark Alyssa Y, Niewiarowski Peter H, Dhinojwala A. 2021 Direct evidence of acid–base interactions in gecko adhesion. *Sci. Adv.* **7**, eabd9410. (doi:10.1126/sciadv.abd9410)
  31. Baio JE, Spinner M, Jaye C, Fischer DA, Gorb SN, Weidner T. 2015 Evidence of a molecular boundary lubricant at snakeskin surfaces. *J. R. Soc. Interface* **12**, 20150817. (doi:10.1098/rsif.2015.0817)
  32. Alibardi L. 2020 Immunolocalization of corneous proteins including a serine-tyrosine-rich beta-protein in the adhesive pads in the tokay gecko. *Microsc. Res. Tech.* **83**, 889–900. (doi:10.1002/jemt.23483)
  33. Roberts JB, Lillywhite HB. 1980 Lipid barrier to water exchange in reptile epidermis. *Science* **207**, 1077–1079. (doi:10.1126/science.207.4435.1077)
  34. Lillywhite HB, Menon JG, Menon GK, Sheehy III CM, Tu MC. 2009 Water exchange and permeability properties of the skin in three species of amphibious sea snakes (*Laticauda* spp.). *J. Exp. Biol.* **212**, 1921–1929. (doi:10.1242/jeb.028704)
  35. Ripamonti A, Alibardi L, Falini G, Fermani S, Gazzano M. 2009 Keratin–lipid structural organization in the corneous layer of snake. *Biopolymers* **91**, 1172–1181. (doi:10.1002/bip.21184)
  36. Sweeney TM, Downing DT. 1970 The role of lipids in the epidermal barrier to water diffusion. *J. Invest. Dermatol.* **55**, 135–140. (doi:10.1111/1523-1747.ep12291678)
  37. Heim M, Elsner MB, Scheibel T. 2013 Lipid-specific beta-sheet formation in a mussel byssus protein domain. *Biomacromolecules* **14**, 3238–3245. (doi:10.1021/bm400860y)
  38. Gorb SN. 1998 The design of the fly adhesive pad: distal tenent setae are adapted to the delivery of an adhesive secretion. *Proc. R. Soc. Lond. B* **265**, 747–752. (doi:10.1098/rspb.1998.0356)
  39. Gorb SN. 2001 *Attachment devices of insect cuticle*. Dordrecht, The Netherlands: Kluwer Academic.
  40. Vötsch W, Nicholson G, Müller R, Stierhof YD, Gorb SN, Schwarz U. 2002 Chemical composition of the attachment pad secretion of the locust *Locusta migratoria*. *Insect Biochem. Mol. Biol.* **32**, 1605–1613. (doi:10.1016/S0965-1748(02)00098-X)
  41. Hiller U. 2009 Water repellence in gecko skin: how do geckos keep clean? In *Functional surfaces in biology: little structures with big effects* (ed. SN Gorb), pp. 47–53. Dordrecht, The Netherlands: Springer.
  42. Stark AY, Badge I, Wucnich NA, Sullivan TW, Niewiarowski PH, Dhinojwala A. 2013 Surface wettability plays a significant role in gecko adhesion underwater. *Proc. Natl Acad. Sci. USA* **110**, 6340–6345. (doi:10.1073/pnas.1219317110)
  43. Stark AY, Subarajan S, Jain D, Niewiarowski PH, Dhinojwala A. 2016 Superhydrophobicity of the gecko toe pad: biological optimization versus laboratory maximization. *Phil. Trans. A Math Phys. Eng. Sci.* **374**, 20160184. (doi:10.1098/rsta.2016.0184)
  44. Riedel J, Vucko MJ, Blomberg SP, Schwarzkopf L. 2020 Skin hydrophobicity as an adaptation for self-cleaning in geckos. *Ecol. Evol.* **10**, 4640–4651. (doi:10.1002/ece3.6218)
  45. Hansen WR, Autumn K. 2005 Evidence for self-cleaning in gecko setae. *Proc. Natl Acad. Sci. USA* **102**, 385–389. (doi:10.1073/pnas.0408304102)
  46. Stöhr J. 1992 *NEXAFS spectroscopy*. Berlin, Germany: Springer-Verlag.
  47. Outka DA, Stöhr J, Rabe JP, Swalen JD. 1988 The orientation of Langmuir–Blodgett monolayers using NEXAFS. *J. Chem. Phys.* **88**, 4076. (doi:10.1063/1.453862)
  48. Sohn KE, Dimitriou MD, Genzer J, Fischer DA, Hawker CJ, Kramer EJ. 2009 Determination of the electron escape depth for NEXAFS spectroscopy. *Langmuir* **25**, 6341–6348. (doi:10.1021/la803951y)
  49. Baio JE, Jaye C, Fischer DA, Weidner T. 2014 High-throughput analysis of molecular orientation on surfaces by NEXAFS imaging of curved sample arrays. *ACS Comb. Sci.* **16**, 449–453. (doi:10.1021/co5001162)
  50. Fischer D, Efimenko K, Bhat R, Sambasivan S, Genzer J. 2004 Mapping surface chemistry and molecular orientation with combinatorial near-edge X-ray absorption fine structure spectroscopy. *Macromol. Rapid Commun.* **25**, 141–149. (doi:10.1002/marc.200300178)
  51. Varol HS *et al.* 2015 Multiscale effects of interfacial polymer confinement in silica nanocomposites. *Macromolecules* **48**, 7929–7937. (doi:10.1021/acs.macromol.5b01111)
  52. Baio JE, Jaye C, Sullivan E, Rasmussen MH, Fischer DA, Gorb S, Weidner T. 2019 NEXAFS imaging to characterize the physio-chemical composition of cuticle from African flower scarab *Eudicella gralli*. *Nat. Commun.* **10**, 4758. (doi:10.1038/s41467-019-12616-5)
  53. Schmäser L, Zhang W, Marx MT, Encinas N, Vollmer D, Gorb S, Baio JE, Räder HJ, Weidner T. 2020 Role of surface chemistry in the superhydrophobicity of the springtail *Orchesella cincta* (Insecta: Collembola). *ACS Appl. Mater. Interfaces* **12**, 12 294–12 304. (doi:10.1021/acsami.9b21615)
  54. Zubavichus Y, Shaporenko A, Grunze M, Zharnikov M. 2008 Is X-ray absorption spectroscopy sensitive to the amino acid composition of functional proteins? *J. Phys. Chem. B* **112**, 4478–4480. (doi:10.1021/jp801248n)
  55. West JD, Zhu Y, Saem S, Moran-Mirabal J, Hitchcock AP. 2017 X-ray absorption spectroscopy and spectromicroscopy of supported lipid bilayers.

- J. Phys. Chem. B* **121**, 4492–4501. (doi:10.1021/acs.jpcc.7b02646)
56. Rivard C, Bakan B, Boulogne C, Elmorjani K, Swaraj S, Belkhou R, Marion D. 2019 Spatial distribution of starch, proteins and lipids in maize endosperm probed by scanning transmission X-ray microscopy. *J. Spectral Imaging* **8**, a21. (doi:10.1255/jsi.2019.a21)
57. Gordon ML, Cooper G, Morin C, Araki T, Turci CC, Kaznatcheev K, Hitchcock AP. 2003 Inner-shell excitation spectroscopy of the peptide bond: comparison of the C 1s, N 1s, and O 1s spectra of glycine, glycyl-glycine, and glycyglycyl-glycine. *J. Phys. Chem. A* **107**, 6144–6159. (doi:10.1021/jp0344390)
58. Zubavichus Y, Shaporenko A, Grunze M, Zharnikov M. 2005 Innershell absorption spectroscopy of amino acids at all relevant absorption edges. *J. Phys. Chem. A* **109**, 6998–7000. (doi:10.1021/jp0535846)
59. Weidner T, Apte J, Gamble LJ, Castner DG. 2010 Probing the orientation and conformation of  $\alpha$ -helix and  $\beta$ -strand model peptides on self-assembled monolayers using sum frequency generation and NEXAFS spectroscopy. *Langmuir* **26**, 3433–3440. (doi:10.1021/la903267x)
60. Zharnikov M, Frey S, Heister K, Grunze M. 2002 An extension of the mean free path approach to X-ray absorption spectroscopy. *J. Electron. Spectrosc. Relat. Phenom.* **124**, 15–24. (doi:10.1016/S0368-2048(02)00004-X)
61. Dertinger T, von der Hocht I, Benda A, Hof M, Enderlein J. 2006 Surface sticking and lateral diffusion of lipids in supported bilayers. *Langmuir* **22**, 9339–9344. (doi:10.1021/la061389s)
62. Rasmussen MH, Holler KR, Baio JE, Jaye C, Fischer DA, Gorb SN, Weidner T. 2022 Evidence that gecko setae are coated with an ordered nanometre-thin lipid film. FigShare. (doi:10.6084/m9.figshare.c.6049219)